Evaluation of Myelopathy and Radiculopathy

18

Lubdha M. Shah and Jeffrey S. Ross

Abstract

Myelopathy and radiculopathy can be due to extrinsic causes, most often degenerative in origin. Imaging can elucidate an often-confusing clinical picture to guide management and provide prognostic information. For intrinsic causes of myelopathy, the differential diagnosis categories include demyelination, inflammation, infection, vascular, and neoplasm. The combination of clinical symptoms, timing of presentation, and imaging features can help narrow the differential diagnosis.

Keywords

Myelopathy · Radiculopathy · MRI · CT · Degenerative
Inflammation · Demyelination · Infection · Neoplasm
Vascular · Hematoma · Metabolic

Learning Objectives

- Explain the clinical differences between myelopathy and radiculopathy to help develop the appropriate differential diagnosis.
- Review the pathophysiology of degenerative changes that result in myelopathy and/or radiculopathy.
- Describe the etiologies that result in extrinsic myelopathy.
- Discuss differentiating imaging features of inflammatory, infectious, vascular, and metabolic spinal cord pathologies.

L. M. Shah (✉)
Department of Radiology, University of Utah,
Salt Lake City, UT, USA
e-mail: lubdha.shah@hsc.utah.edu

J. S. Ross
Department of Radiology, Mayo Clinic, Phoenix, AZ, USA
e-mail: Ross.Jeffrey1@mayo.edu

18.1 Clinical Presentation

Spinal cord lesions may result in the clinical findings of myelopathy, presenting as abnormalities in motor, sensory, and autonomic pathways which can be manifest as paresthesias, decreased dexterity, changes in mobility, or frequent falls. When a patient has a lesion either intrinsically or extrinsically affecting a spinal nerve or plexus, they may present with radiculopathy, which includes pain, weakness, reflex changes, and sensory loss in the specific nerve distribution. The lumbosacral cauda equina nerve roots are the peripheral transition distal to the conus medullaris of the central nervous system. As these two areas are in close-proximity, lesions in one area can affect the function of the other.

18.2 Myelopathy

Lesions that cause myelopathy may either be extrinsic compressive or intrinsic non-compressive to the spinal cord. Although many etiologies can have overlapping imaging appearances, clinical history and demographics are critical to narrow the possible etiologies. The pattern of spinal cord involvement is also important to consider and can help in developing a differential diagnosis.

Key Point

- When a patient presents with symptoms of myelopathy, it is important to consider both extrinsic compressive lesions, which may necessitate surgical intervention, and pathologies that involve the spinal cord parenchyma.

J. Hodler et al. (eds.), *Diseases of the Brain, Head and Neck, Spine 2024-2027*, IDKD Springer Series,
https://doi.org/10.1007/978-3-031-50675-8_18

18.2.1 Extrinsic

Degenerative cervical myelopathy (DCM) is a very common cause of myelopathy due to extrinsic compression. DCM reflects age-related chronic spinal cord injury through degenerative changes of the spinal axis with both static and dynamic contributing factors. Disc degeneration includes loss of disc height, disc herniations, osteophyte formation, and thickening of the ligamentum flavum, which may result in loss of cervical lordosis. There may be instability or hypermobility due to the ligamentous laxity, which may put stress on the facet and uncovertebral joints with resultant hypertrophy. The osteophytes and buckled ligaments may cause static compression of the spinal cord, which is further exacerbated by the straightened or kyphotic alignment with stretching of the spinal cord while the hypermobility contributes to dynamic injury. Regional and local spinal cord perfusion are compromised in DCM. The blood–spinal cord barrier may be disrupted with chronic ischemia followed by an influx of inflammatory cells into the spinal cord parenchyma with subsequent inflammation [1].

DCM pathophysiology is reflected in the imaging appearance. Patients with DCM may have hyperintensity within the cord on T2WI (T2-weighted imaging) and, less commonly, hypointensity on T1WI (T1-weighted imaging) in the region of the compression. The prevalence of hyperintense signal on T2WI among patients with clinically confirmed DCM has been reported within the range of 58–85%. T2WI hyperintensity may be strongly hyperintense and well-circumscribed or less hyperintense and diffuse (without a clear margin). It is thought that these changes represent different states of pathology and have different recovery potentials [2]. DCM may also have a distinct pattern of contrast enhancement: a transverse axial or pancake-like enhancement at or just caudal to the site of maximal stenosis and at the rostrocaudal midpoint of a spindle-shaped T2 hyperintensity (Fig. 18.1). This enhancement can persist for months, even years, following surgical decompression [3]. Clinical correlation is essential for the diagnosis of DCM since cervical degenerative disc disease is ubiquitous. One study found that up to 60% of asymptomatic individuals older than 40 years of age can show degenerative changes on MRI [4], while another showed that up to 90% over the age of 60 years and associated with age and degeneration in other spinal segments [5].

Key Point

- DCM may have a distinct pancake-like enhancement at the site of maximal stenosis.

Epidural lesions such as spontaneous epidural hematoma (SEH) and epidural abscess may cause neurologic deficits due extrinsic compression. SEH is the atraumatic accumulation of blood in the epidural space due to multiple potential etiologies such as coagulopathy, anticoagulation, neoplasm, vascular malformation, hypertension, increased intra-abdominal or intra-thoracic pressure (such as straining, sneezing, lifting), and idiopathic (40–60% of cases). Patients with spontaneous spinal epidural hematoma typically present with acute onset of severe back pain and rapidly develop signs of compression of the spinal cord or cauda equina nerve roots. The pathophysiology is hypothesized to be due to venous bleeding [6] or, less likely, arterial bleeding. CT may reveal hyperdense blood products effacing the hypodense fat in the epidural space. Similarly on MRI, effacement of the T1 hyperintense epidural fat is a helpful clue to the epidural location. MR imaging appearance of SEH changes over time as the hemoglobin evolves (Table 18.1). SEH may demonstrate mild peripheral enhancement [7] (Fig. 18.2).

Epidural abscess may occur due to hematogenous dissemination, direct inoculation, or extension from contiguous infected tissues, such as discitis-osteomyelitis. Patients may present with neck or back pain and fever. The severity of neurological deficits depends on the extent of cord compression. An epidural abscess will show central nonenhancing fluid signal intensity, with irregular and thick peripheral enhancement. Diffusion-weighted imaging (DWI) can be extremely helpful in the diagnosis of spinal epidural abscess, as it is in the brain, showing markedly increased signal with infection (Fig. 18.3). Although blood products may also show increased signal on DWI [8], imaging clues such as paraspinal edema/enhancement/abscess or bone marrow edema/enhancement may point to infectious process. The appearance of epidural phlegmon is usually amorphous T1 isointense to hypointense, and T2 hyperintense fluid which effaces the epidural fat. Phlegmon shows diffuse enhancement while abscess will demonstrate peripheral enhancement.

Neoplastic lesions involving the extradural space, originating in the osseous structures or the epidural compartment, can compress the spinal cord and nerve roots. A pathologic fracture with retropulsion of bone can result in cauda equina syndrome (e.g., urinary retention urinary/fecal incontinence, saddle anesthesia, lower extremity weakness, back and/or leg pain). Imaging features on conventional MRI that favor a pathologic fracture include abnormal posterior element signal, epidural or paravertebral soft tissue mass, geographic replacement of normal marrow signal, irregular margins, and bowing of the posterior cortex [9] (Fig. 18.4). The acutely impacted spinal cord may exhibit intramedullary T2 hyperintensity due to edema.

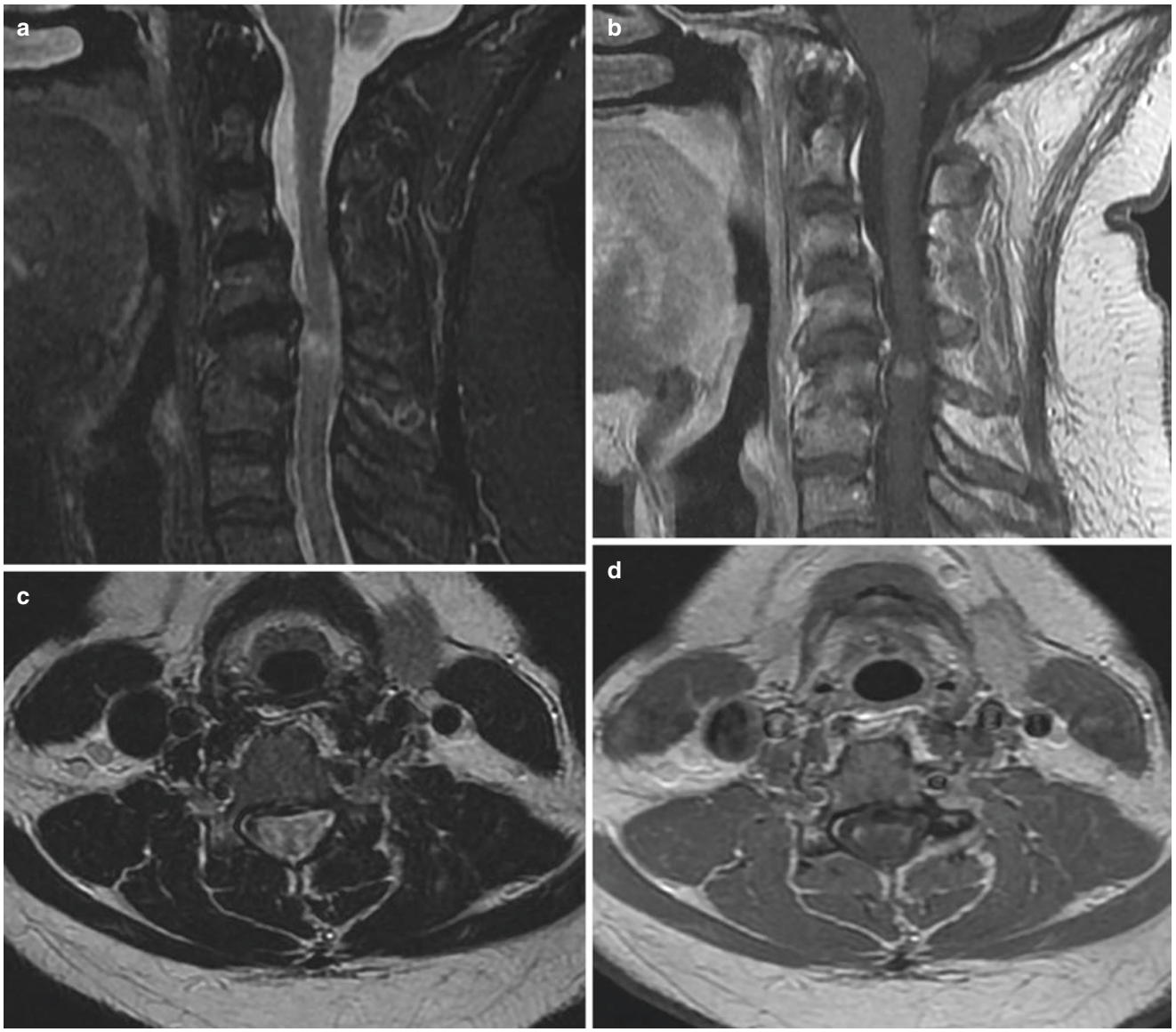

Fig. 18.1 (**a**) Sagittal and (**c**) axial T2WI shows focal intramedullary hyperintensity at the C5 level. (**b**) Sagittal contrast-enhanced T1WI demonstrates horizontal, "pancake-like" enhancement at this level, characteristic of DCM. (**d**) Axial contrast-enhanced T1WI shows irregular, peripheral enhancement

Table 18.1 MRI of spontaneous epidural hematoma

Age	MRI appearance
Acute	Nonspecific fluid intensity: T1 isointense, T2 heterogeneous hyperintense
Early subacute	T1 hyperintense, T2 hypointense
Late subacute	T1 hyperintense, T2 hyperintense
Chronic	T1 hypointense, T2 hypointense

Key Point

- MRI features of a pathologic fracture include abnormal posterior element signal, soft tissue mass, abnormal marrow signal, irregular margins, and bowing of the posterior cortex. On the other hand, an osteoporotic fracture shows normal posterior element signal intensity, retropulsion of the posterior cortex, linear horizontal hypointense T1/T2 band, fluid sign, and normal enhancement relative to adjacent vertebrae.

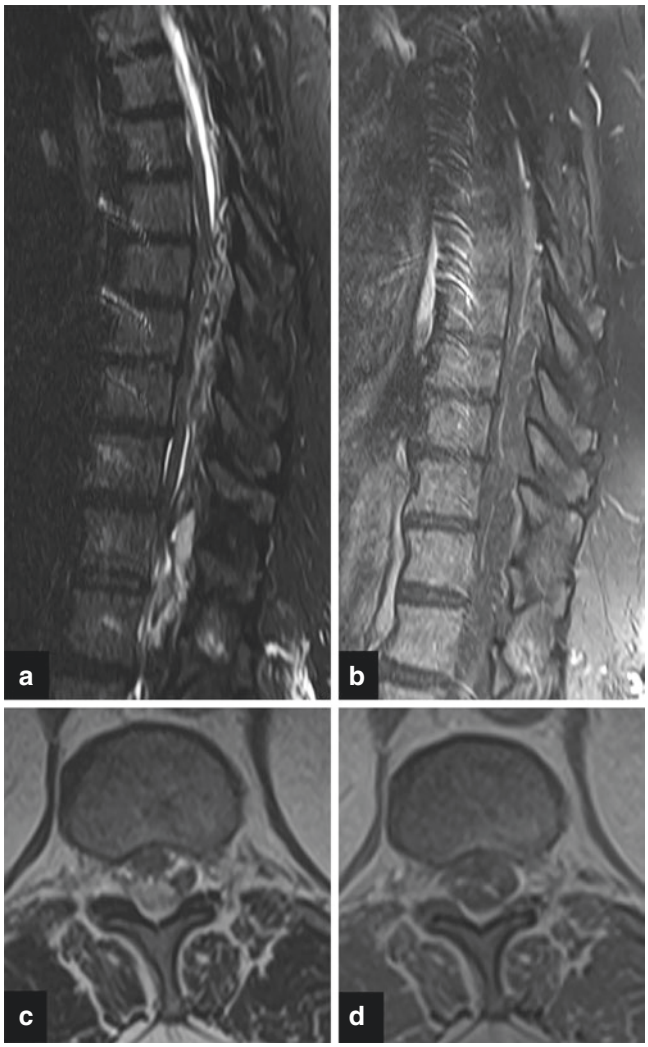

Fig. 18.2 (**a**) Sagittal STIR MRI shows heterogeneous hyper-/hypointense collection in the dorsal epidural space. (**c**) Axial T2WI demonstrates anterior displacement and mass effect on the thecal sac by the SEH. (**b**) Sagittal and (**d**) axial contrast-enhanced T1WI shows peripheral enhancement of the dorsal epidural collection

Intradural extramedullary lesions can also impinge upon the spinal cord, resulting in myelopathic symptoms. Meningiomas are common intradural extramedullary spinal lesions, which arise from the arachnoid meningothelial cells, are commonly in the thoracic segment (80%), and shows a female predilection [10]. Although the majority of meningiomas are World Health Organization grade I, they are symptomatic because of spinal cord or nerve root compression. Patients may experience gait ataxia, localized or radicular pain, and sensorimotor deficits. On MRI, meningiomas demonstrate T1 iso-/hypointensity, slight T2 hyperintensity, and avid enhancement (Fig. 18.5). Tapered enhancing margins, (dural tail) can be a helpful imaging clue. Susceptibility artifacts may be present if there is calcification. Densely calcified lesions may be confusing on post-contrast images as they tend to show very little central enhancement. The compressed spinal cord will exhibit intramedullary T2 hyperintensity due to edema and gliosis in the setting of chronic impingement.

Ventral displacement of the spinal cord may reflect a variety of lesions which may be anterior or posterior to the cord. Primary posterior lesions include arachnoid web and arachnoid cyst. A ventral lesion is transdural cord herniation. Arachnoid webs are an intradural extramedullary transverse bands of arachnoid tissue that extends to the dorsal surface of the spinal cord, causing mass effect and dorsal cord indentation. Altered CSF flow dynamics from this web may result in cord edema which may eventually develop into syringomyelia. Patients may present with back pain and upper and lower extremity weakness and numbness. On MRI or CT myelogram, the arachnoid web causes a characteristic focal dorsal indentation of the dorsal spinal cord, "scalpel sign" [11] (Fig. 18.6a, b, c). Spinal cord herniation is considered when there is focal ventral protrusion of the spinal cord is a patient with back pain and motor and sensory deficits. The "C-shape" of the dorsal indentation favors spinal cord herniation [12] (Fig. 18.6d, e). Although most spinal cord herniation cases are idiopathic, other uncommon etiologies include prior trauma, dural rent due to disc protrusion, congenital dural defect, or inflammatory process leading to adhesion of the cord to the ventral dura.

18.2.2 Intrinsic

Non-compressive lesions affecting the spinal cord parenchyma can result in myelopathy. The MRI pattern, particularly on the T2WI sequences, can be helpful in developing differential diagnosis. However, the temporal presentation and clinical signs and symptoms are crucial to narrow the differential considerations. For example, infectious processes and vascular injuries tend to present acutely. On the other hand, if the patient's myelopathic symptoms are insidious in onset or progressive, differential considerations include metabolic or inflammatory processes and intramedullary neoplasm.

Demyelinating diseases may have characteristic imaging features on brain and spine MRI that may be helpful in distinguishing between the different demyelinating diseases (Fig. 18.7). Multiple sclerosis (MS) is the prototypical demyelinating disease, characterized by waxing and waning symptoms related to brain and spinal lesions. The spinal cord, particularly the cervical segment, is affected in more than 90% of patients with clinically definite MS. The classic spinal cord MS plaque is an ovoid T2 hyperintense lesion, spanning less than two vertebral bodies craniocaudally, affecting less than half the cross-section of the cord, and located in the posterior and posterolateral cord [13]. Active

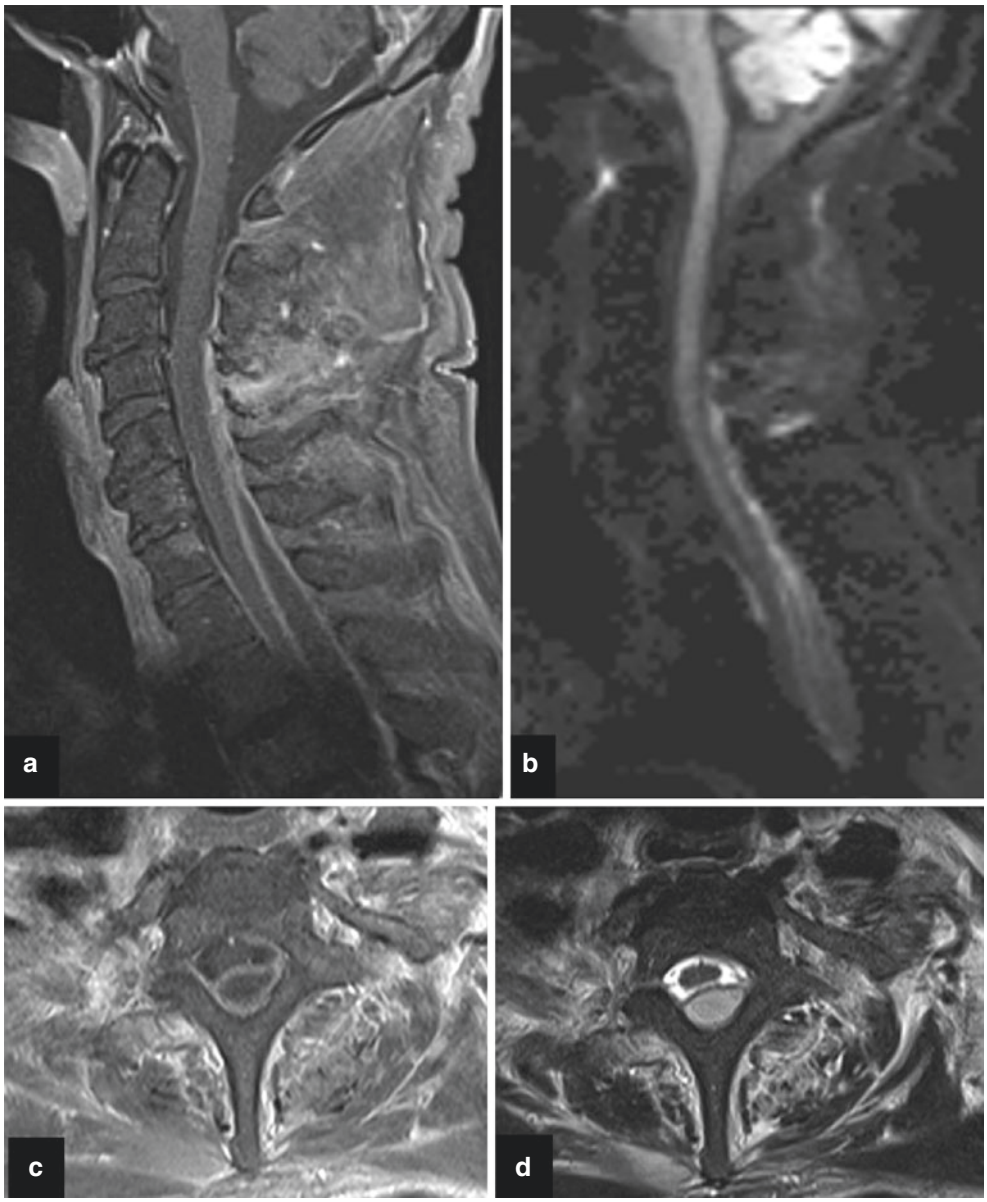

Fig. 18.3 (**a**) Sagittal contrast-enhanced T1WI demonstrates a peripherally enhancing fluid collection in the patient with increasing upper back pain and mild leukocytosis. (**b**) Sagittal DWI shows hyperintensity in this collection due to the purulent material. (**c**) Axial contrast-enhanced T1WI and (**d**) T2WI show compression and anterior displacement by this epidural abscess

lesions may show mild swelling, and transient breakdown of the blood–cord barrier can result in lesion enhancement of the lesion. Chronic disease may result in spinal cord atrophy with focal areas of gliosis due to axonal loss.

Other demyelinating lesions involve longer segments of the spinal cord. Acute disseminated encephalomyelitis (ADEM) is a monophasic illness that may occur after viral illness or vaccination due to autoimmune reaction to myelin basic protein. ADEM lesions are poorly marginated, longer in the craniocaudal extent, involve a greater cross-section of the spinal cord, variably enhance, and tend to involve the thoracic spinal cord.

Neuromyelitis optica spectrum disorder (NMOSD) is a demyelinating process that involves the optic nerves and spinal cord, with brain involvement concentrated in the distribution of the aquaporin four channels (e.g., hypothalamus, periaqueductal gray matter, area postrema). The spinal cord lesions are classically greater than three vertebral bodies in craniocaudal extent (longitudinally extensive), involve the central gray matter and greater than 2/3 of the cord cross-section, and frequently extend cephalad to the medulla [14]. Some lesions have heterogeneous internal foci of T2 hyperintensity, described as "bright spotty lesions" [15]. There may be variable enhancement and tumefactive cord expansion.

Myelin Oligodendrocyte Glycoprotein IgG Associated Disease (MOGAD) is a distinct severe demyelinating pathology related to a glycoprotein on the myelin surface, which may be confused with NMOSD. Children older than 9 years of age and adults present with optic neuritis, usually bilateral, longitudinally extensive transverse myelitis, and brainstem lesions [16]. Conus medullaris predilection [17], central

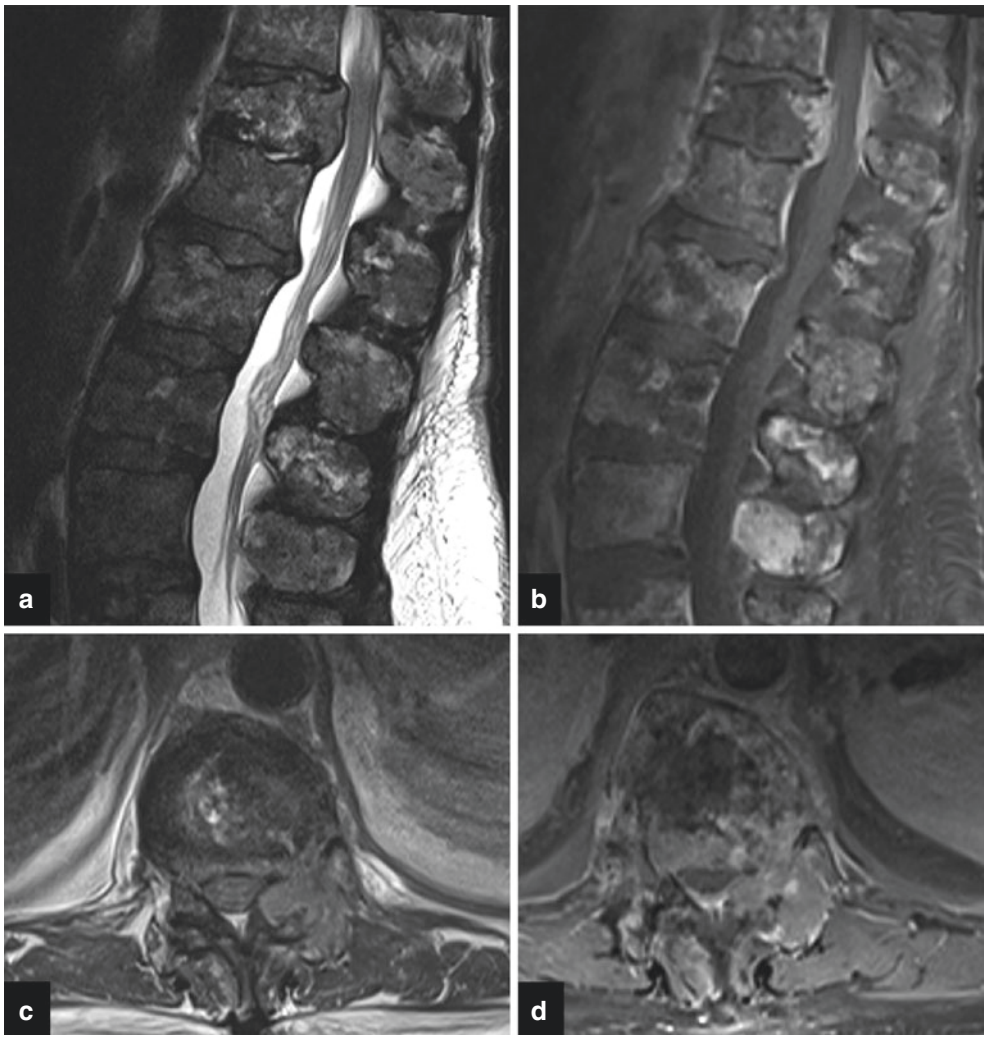

Fig. 18.4 (**a**) Sagittal T2WI and (**b**) contrast-enhanced T1WI show multiple osseous metastases involving the lower thoracic and lumbar spine with a pathological fracture of T12. (**c**) Axial T2WI and (**d**) axial contrast-enhanced T1WI demonstrate bowing of the posterior cortex and the epidural extension causing severe narrowing of the spinal subarachnoid space and compression of the distal spinal cord

grey matter involvement, and lack of enhancement are more characteristic features of MOGAD.

Sarcoidosis is chronic idiopathic, multisystem inflammatory disorder which can involve the central nervous system in up 25% of patients [18], with intramedullary involvement in less than 1% of cases [19]. T2WI demonstrates mildly enlargement of the spinal cord with extensive hyperintensity. On contrast-enhanced T1WI, there may be linear leptomeningeal enhancement along pial surface in early phases. Intramedullary involvement occurs due to centripetal spread through perivascular spaces. Central canal enhancement with a "trident sign" can be seem with subacute myelitis and manifest as dorsal cord involvement with central and lateral extensions [20] (Fig. 18.8).

Key Point

- Neurosarcoidosis can have a characteristic pattern of central and lateral enhancement, "trident sign" due to centripetal spread through perivascular spaces.

Infectious myelopathies may result from direct invasion by the pathogen or as a parainfectious immune-mediated process. Contrast-enhanced MRI will reveal patterns of spinal cord abnormality including central (segmental or longitudinally extensive), eccentric tract-specific (lateral columns, posterior columns), ventral horn, and irregular/mass-like, which may help to narrow the differential diagnosis. Overlapping imaging patterns may be seen, and, in some cases, the spinal cord may appear normal on MRI.

Numerous viruses can cause infectious myelitis, some of which are particularly neurotropic such as herpesviruses, flaviviruses, and enteroviruses. Several enteroviruses are implicated in myelitis (e.g., enterovirus 71, coxsackieviruses, echovirus, and poliovirus) and have a predilection for ventral horn cell involvement. On MRI, there will be abnormal signal within the ventral nerve roots (unilateral or bilateral). With enterovirus 71, MRI typically shows segmental or longitudinally extensive T2 hyperintensity centered in the ventral horns with variable enhancement (Fig. 18.9). A central longitudinally extensive transverse myelitis pattern may also be seen less frequently and portends a worse prognosis [21].

Fig. 18.5 (**a**) Sagittal T2WI shows a mildly hypointense, well-circumscribed intradural extramedullary lesion anteriorly displacing the mid-thoracic spinal cord. (**c**) Axial T2WI demonstrates marked compression of the spinal cord by this lesion. (**b**) Sagittal and (**d**) axial contrast-enhanced T1WI display the avid enhancement of the meningioma

Similarly, enterovirus D68 infections result in confluent longitudinally extensive T2 hyperintensity of the cervical spinal cord gray matter, with involvement of dorsal pontine tegmentum and ventral pons. Central intramedullary and nerve root enhancement has also been described [21]. Approximately 5–10% of neuroinvasive cases of West Nile virus (WNV) are associated with myelitis, presenting with acute flaccid paralysis. The MRI appearance in WNV is quite variable and may be unremarkable. WNV also has a predilection for ventral horn cell involvement, which may present as abnormal signal within the ventral cord, sometimes with associated ventral nerve root enhancement.

Other neurotropic viruses can have distinct patterns of spinal cord involvement. MRI in patients with Human Immunodeficiency Virus (HIV) demonstrates symmetric nonenhancing T2 hyperintensity within the posterior columns, most commonly involving the thoracic spinal cord (Fig. 18.10). The pathologic process is vacuolar myelopathy and parallels the AIDS dementia complex spectrum, i.e., seen in later stages of the disease. The posterior column

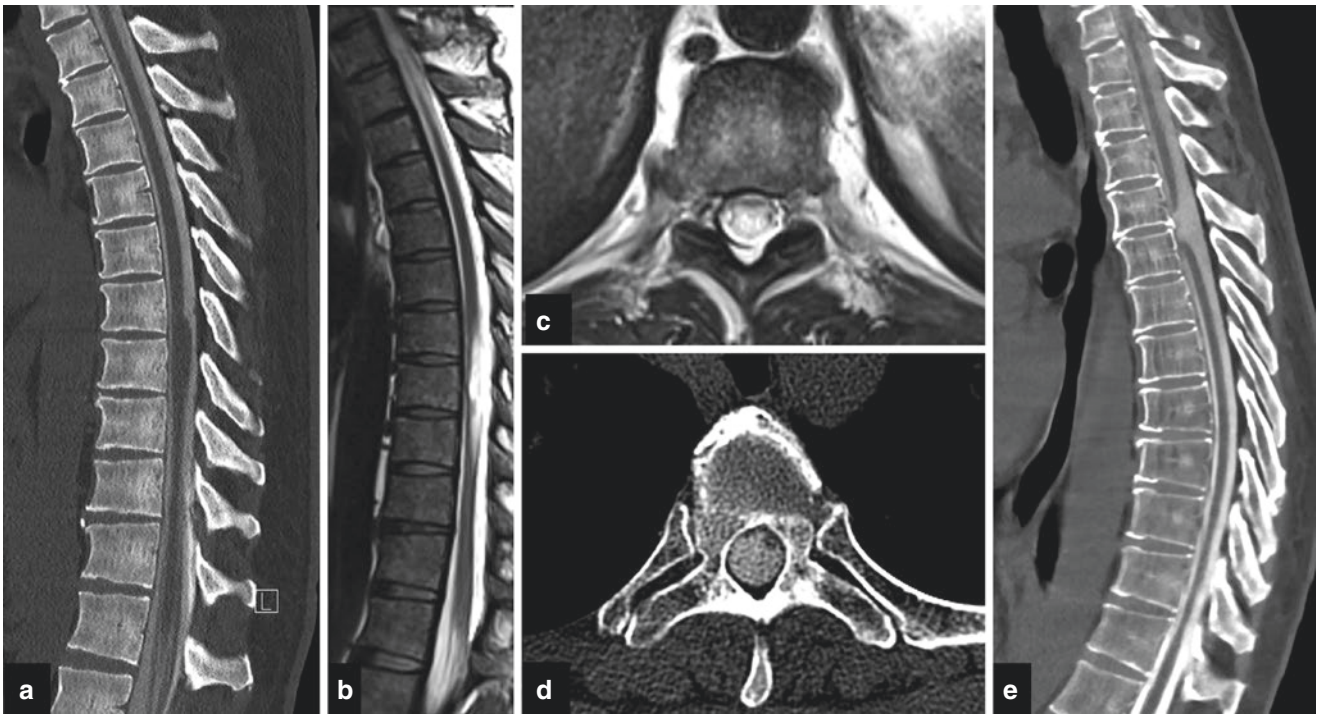

Fig. 18.6 (**a**) Sagittal CT myelogram and (**b**) sagittal T2WI demonstrates the dorsal indentation in the mid-thoracic spine (scalpel sign) due to an arachnoid web. (**c**) Axial T2WI shows intramedullary edema. (**d**) Axial CT myelogram demonstrates ventral herniation of the spinal cord through a dural defect. (**e**) Sagittal CT myelogram shows the "C-shaped" morphology suggestive of cord herniation

involvement explains the symptoms of a slowly progressive spastic paraparesis, impaired vibratory and position sense, and urinary urgency. In patients with varicella zoster virus myelitis, MRI reveals T2 hyperintensity in the dorsal horn and posterior column. The virus enters the spinal cord dorsal root and posterior column sand can extend vertically. Patients present with a skin rash then after a few days to weeks, the myelopathic symptoms begin. The skin rash is typically at the level of the spinal cord lesions.

Arterial vascular pathologies of the spinal cord can cause neurologic deficits. Clinical presentation of spinal cord ischemia is usually abrupt and depends mainly on the location and extent of the infarction. The maximal symptomatology is reached within 12 h for 50% of patients and within 72 h for most patients [22]. Spinal cord infarctions, predominantly in the anterior spinal artery distribution, are commonly due to atherosclerosis, hypertension, diabetes, fibrocartilaginous emboli, and other various vaso-occlusive etiologies. Acutely, DWI will show hyperintensity with corresponding hyperintensity on the apparent diffusion coefficient (ADC) images in the affected region. There will be hyperintense signal on T2WI and STIR and isointensity on T1WI. When the anterior spinal artery territory is affected, abnormal signal is seen in the ventral horns and the adjacent white matter (Fig. 18.11). Associated edema results in slight cord enlargement. Patchy enhancement may be seen in the subacute phase due to breakdown of the blood–cord barrier.

Spinal vascular malformations can present with acute or progressive symptoms, depending on the type of vascular shunt. Multiple different naming conventions have been applied to the wide variety of spinal vascular malformations, but in general the most common types can be defined as (1) Spinal dural arteriovenous fistula (SDAVF); (2) Glomus arteriovenous malformations (AVM); and (3) Perimedullary AVFs. SDAVFs are slow-flow lesions and account for 70% of all spinal vascular shunts. Classically, the presentation is that of an older male (55–60 years) with a history of nonspecific progressive myelopathic symptoms. Most (~80%) of SDAVFs are observed along the posterior lower thoracic cord surface between levels T6 and L2. The anomalous intradural communication between a dural artery and radicular vein within the intervertebral foramen results in engorged venous collaterals, producing the angiographic "single coiled vessel" appearance (Fig. 18.12). On T2WI, there are prominent serpentine flow voids overlying the posterior spinal cord. Venous congestion results in intramedullary edema/ T2 hyperintensity and mild cord expansion. Deoxyhemoglobin in dilated capillaries may produce a T2 hypointense rim [23]. There may be patchy intramedullary enhancement due to breakdown of the blood–cord barrier. Patients with a spinal glomus AVM may present with acute or subacute symptoms related to subarachnoid or cord hemorrhage. Similarly, patients with an intradural perimedullary AVF can present with acute neurologic deficits due to subarachnoid hemor-

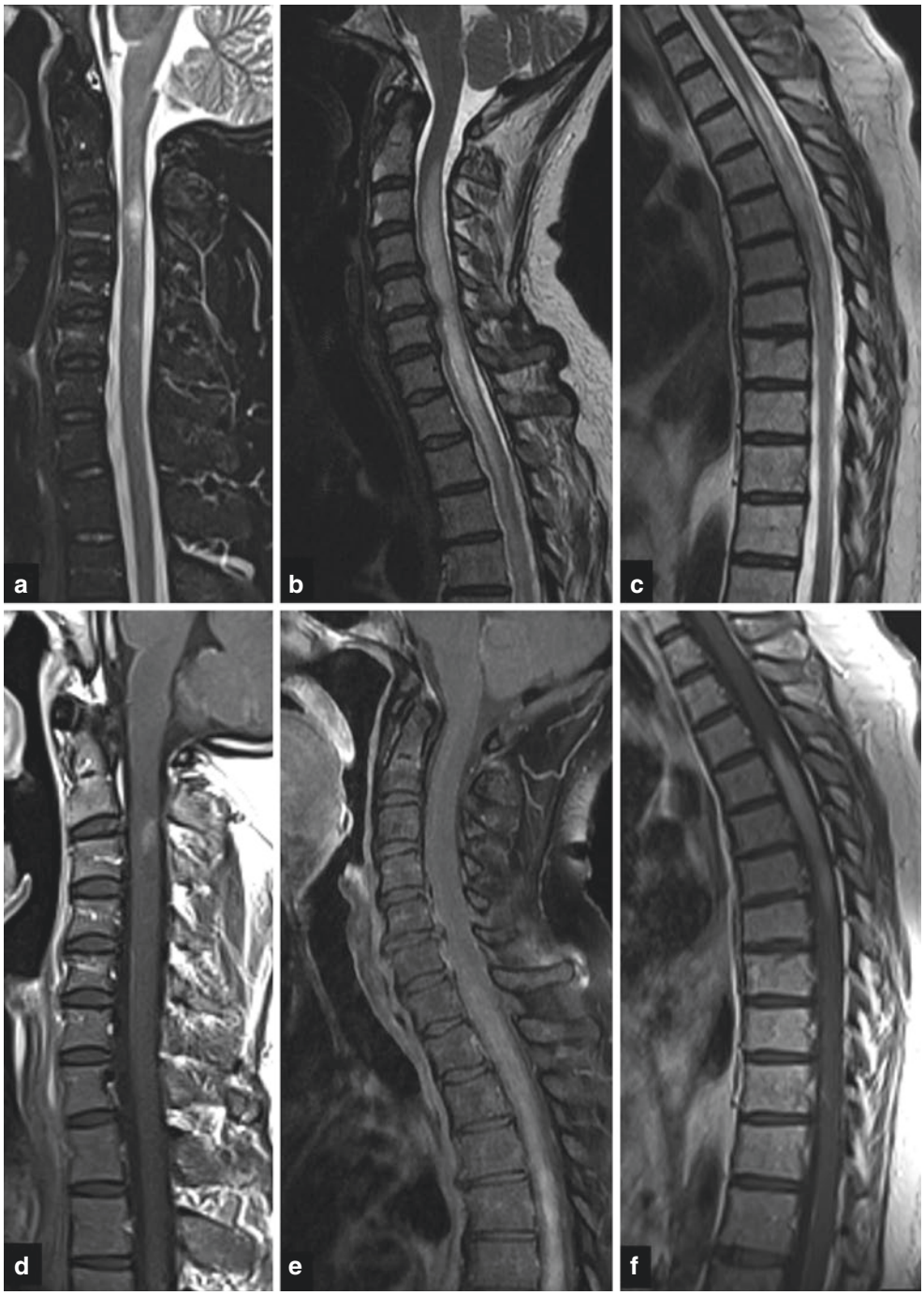

Fig. 18.7 (**a**) Sagittal STIR MRI and (**d**) contrast-enhanced T1WI of the cervical spinal cord show the ovoid lesion of MS, spanning <2 vertebral bodies in length. The lesion demonstrates well-defined enhancement. (**b**) Sagittal T2WI and (**e**) contrast-enhanced T1WI of the cervical spinal cord in a patient with ADEM shows a long segment of intramedullary T2 hyperintensity and patchy, ill-defined enhancement, respectively, and mild cord expansion. This patient had viral prodrome and rapidly processive extremity weakness. (**c**) Sagittal T2WI and (**f**) contrast-enhanced T1WI of the thoracic spinal cord demonstrates a heterogeneously T2 hyperintense lesion involving the mid-thoracic cord with avid "mass-like" enhancement in this patient with NMOSD

rhage or myelopathy related to venous congestion. The spinal glomus AVM nidus shows variable enhancement and may be partially or completely intramedullary with surrounding T2 hyperintensity. There may be radicular venous intra- and perimedullary flow voids and subarachnoid or parenchymal hemorrhage. With intradural perimedullary AVFs, MRI demonstrates prominent perimedullary flow voids typically along the ventral cord surface. Arterial and venous ectasia may cause cord compression. There is variable intramedullary T2 hyperintensity and pial enhancement.

Cavernous malformations are intramedullary lobulated dilated sinusoidal channels of dense capillary-like vessels without intervening neural tissue. While half of the patients with cavernous malformations present with progressive deterioration due to microhemorrhage, gliosis, microcirculatory changes, and partial thrombosis, the other half may have an acute or recurrent presentation due to larger hemorrhage

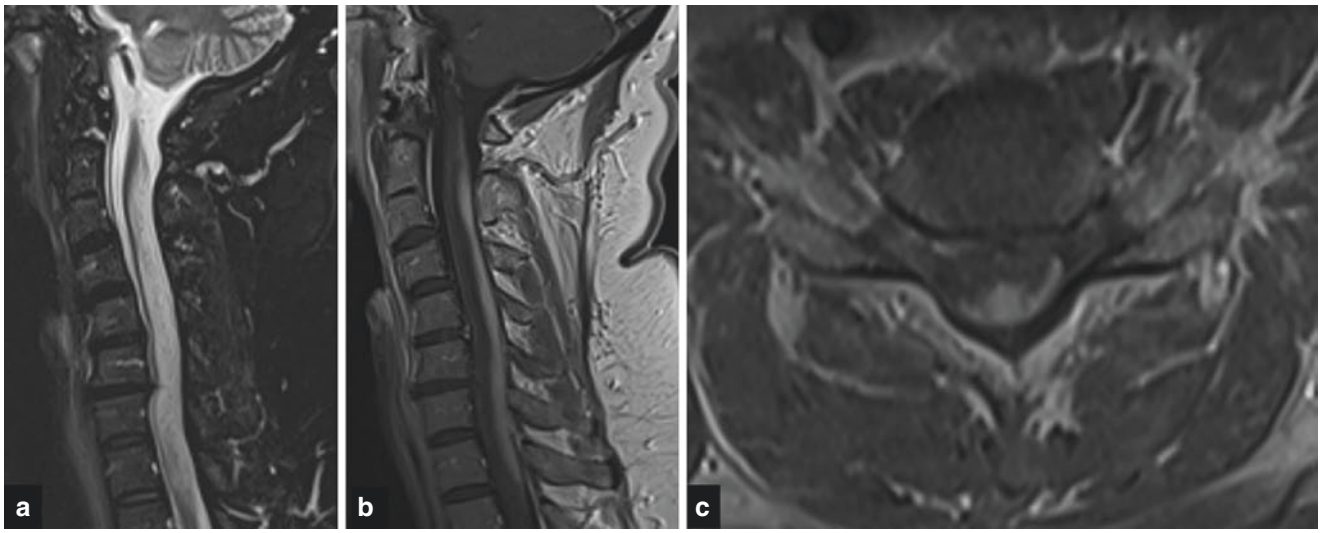

Fig. 18.8 (**a**) Sagittal STIR MRI shows long segmental of cervical cord intramedullary hyperintensity with mild expansion. (**b**) Sagittal contrast-enhanced T1WI demonstrates intramedullary enhancement along the dorsal aspect of the cord. (**c**) Axial contrast-enhanced T1WI illustrates dorsal cord enhancement with central and lateral extensions (trident sign), a finding highly suggestive of neurosarcoidosis

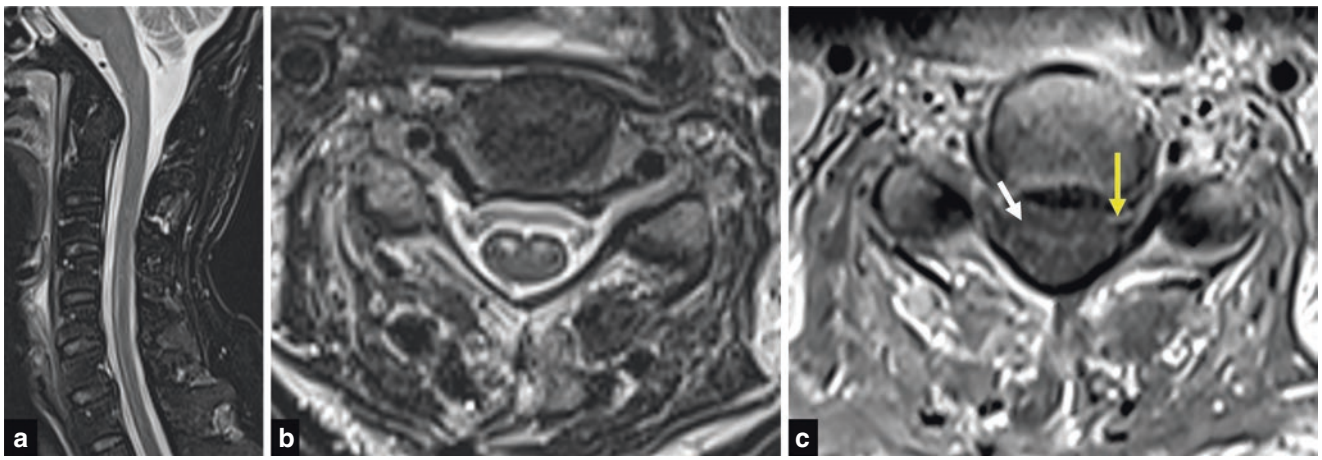

Fig. 18.9 (**a**) Sagittal STIR MRI shows a long segment of hyperintensity in the ventral cord. (**b**) Axial T2WI demonstrates hyperintensity in the ventral horns in this patient with enterovirus 71 myelitis. (**c**) Axial contrast-enhanced T1WI illustrates enhancement in the ventral horns (white arrow) and linear enhancement along the left ventral nerve root (yellow arrow)

within or beyond the capsule of the lesion. The average estimated annual hemorrhage risk of 2.1% [24]. On MRI, spinal cavernous malformations have the typical appearance of circumscribed, multilobulated lesions with heterogeneous T1 and T2 signal intensity and T2 hypointense rim. The heterogenous signal intensities are due to the various ages of blood by-products as well as calcifications and fibrosis (Fig. 18.13).

A variety of metabolic lesions can present with myelopathic symptoms. Subacute combined degeneration (SCD) is the term given for vitamin B12 deficiency that can produce paresthesias initially followed by sensory disturbances, weakness, and spasticity and primarily involves the dorsal and lateral spinal columns. As this is a treatable condition and the symptoms are potentially reversible, awareness of the imaging features is critical. B12 is important for all methylation reactions, including those needed for myelin phospholipids; therefore, its deficiency results in unstable myelin. On MRI, there may be modest expansion of the cervical and thoracic spinal cord and increased signal intensity on T2-weighted images, primarily in the dorsal columns in an inverted "V" configuration (Fig. 18.14). Rarely, there may be mild enhancement due to breakdown of the blood–cord barrier [25]. Other deficiency-related metabolic diseases that can cause T2 hyperintensity in the dorsal and possible lateral columns include acquired copper, folate, vitamin E deficiency, nitrous oxide toxicity (such in substance abuse with inhalation of whipped cream chargers), and intrathecal methotrexate [26].

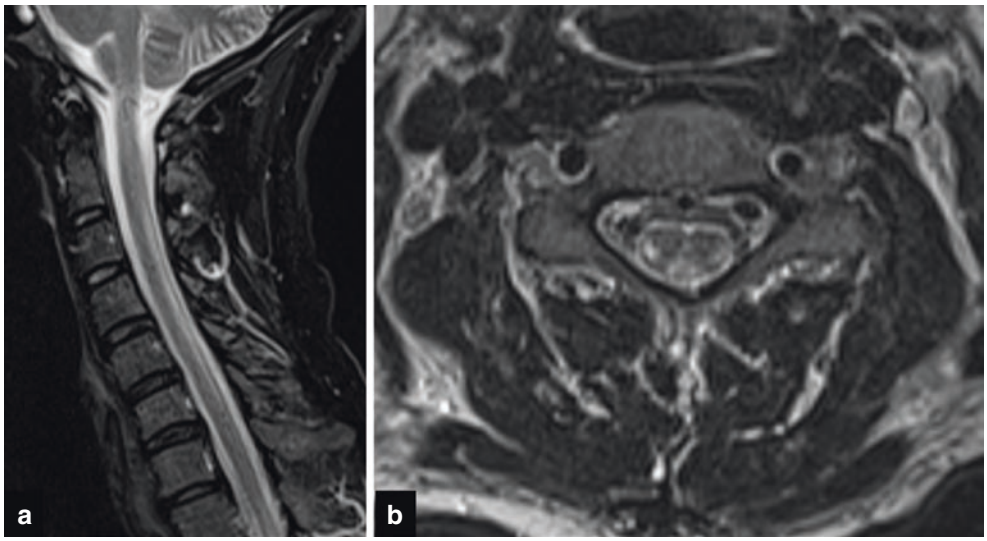

Fig. 18.10 (**a**) Sagittal STIR MRI show intramedullary hyperintensity in the posterior cord. (**b**) Axial T2WI demonstrates abnormal signal in the posterior and lateral columns related to HIV vacuolar myelopathy

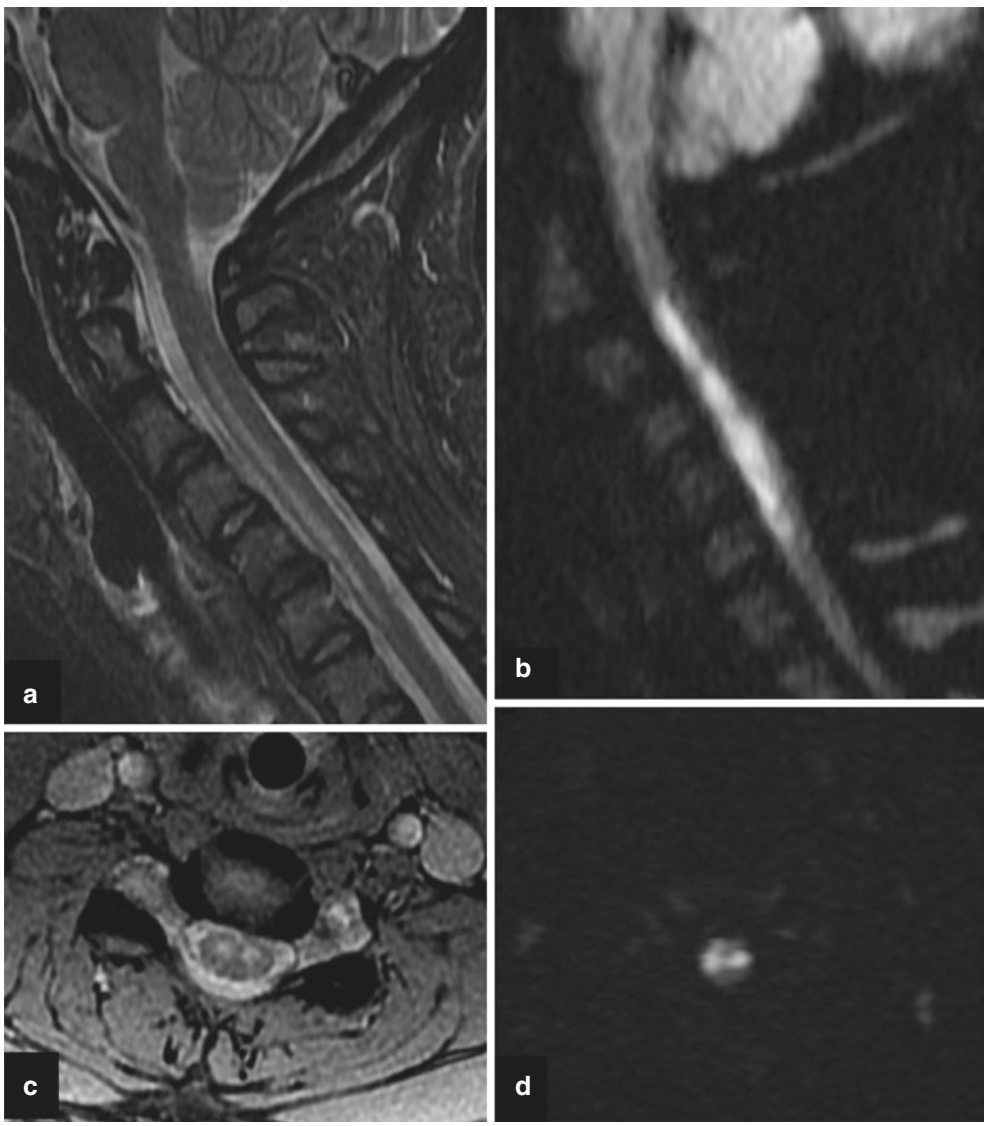

Fig. 18.11 (**a**) Sagittal STIR MRI and (**b**) DWI show anterior cervical cord hyperintensity in this patient with acute onset of extremity weakness related to spinal cord infarction. (**c**) Axial GRE and (**d**) DWI demonstrate hyperintensity in the ventral horns, reflecting anterior spinal artery territory of the ischemic injury

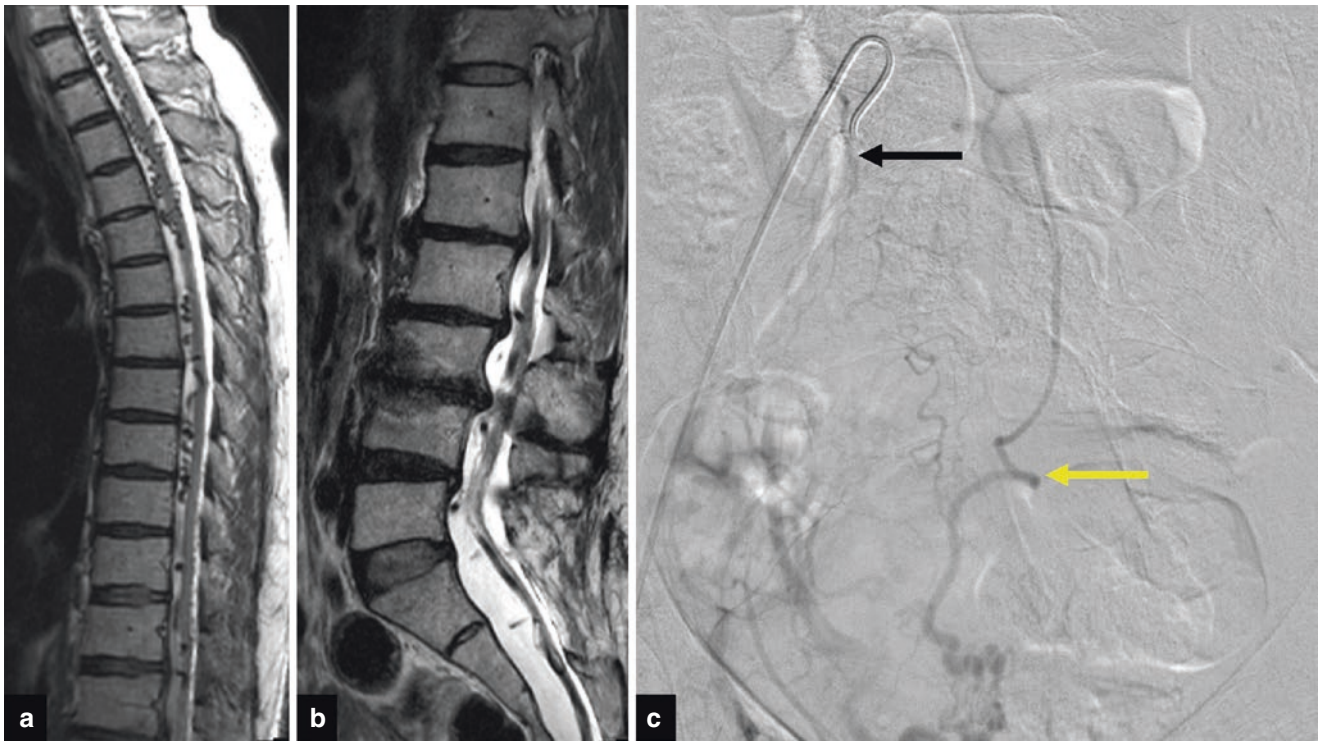

Fig. 18.12 Sagittal T2WI of the (**a**) thoracic and (**b**) lumbar spine demonstrates prominent, serpentine vessels overlying the spinal cord and the cauda equina nerves. (**c**) Frontal digital subtraction angiographic image shows SDAVF arising from lateral sacral arteries (black arrow). Venous drainage is to a dilated perimedullary vein coursing superiorly (yellow arrow)

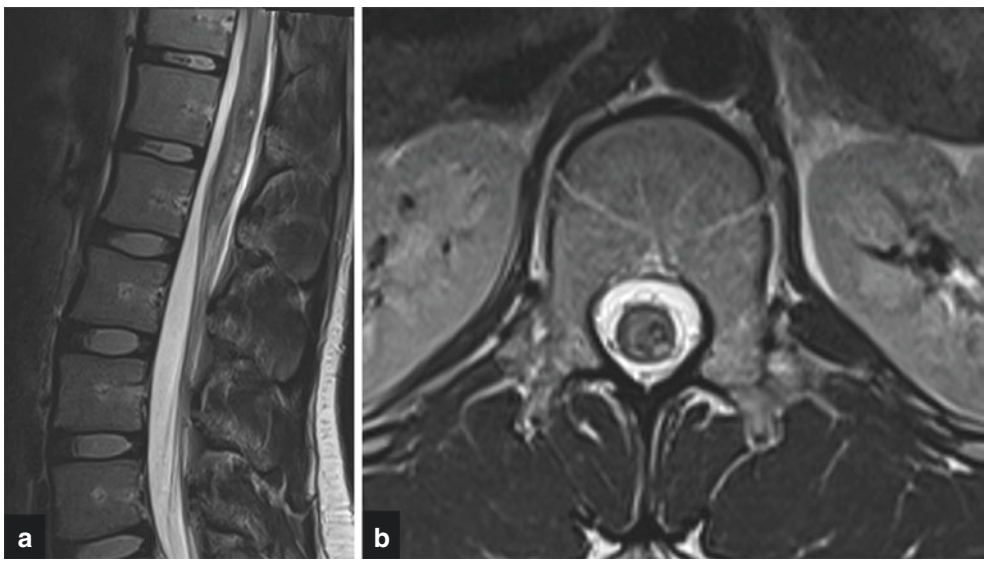

Fig. 18.13 (**a**) Sagittal and (**b**) axial T2WI show a heterogenous intramedullary lesion with a T2 hypointense rim in the distal spinal cord related to a cavernous malformation. Recent intralesional hemorrhage results in mild cord expansion and edema

Key Point

- SCD has the classic appearance of an inverted "V" on T2-weighted MRI.

Imaging features that suggest intramedullary neoplasm as the cause of a patient's subacute/ chronic or progressive neurologic symptoms include abnormal cord signal intensity with focal cord expansion, focal/nodular cord enhancement, hemorrhage, and cord cyst formation. The common primary

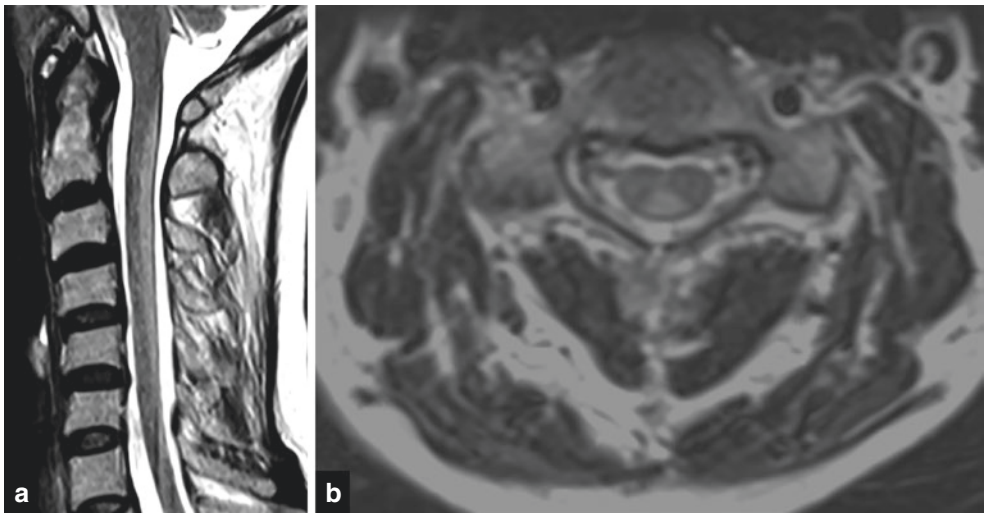

Fig. 18.14 (**a**) Sagittal and (**b**) axial T2WI show hyperintensity in the posterior cervical cord, specifically involving the posterior columns, in this patient with leg and arm numbness due to SCD

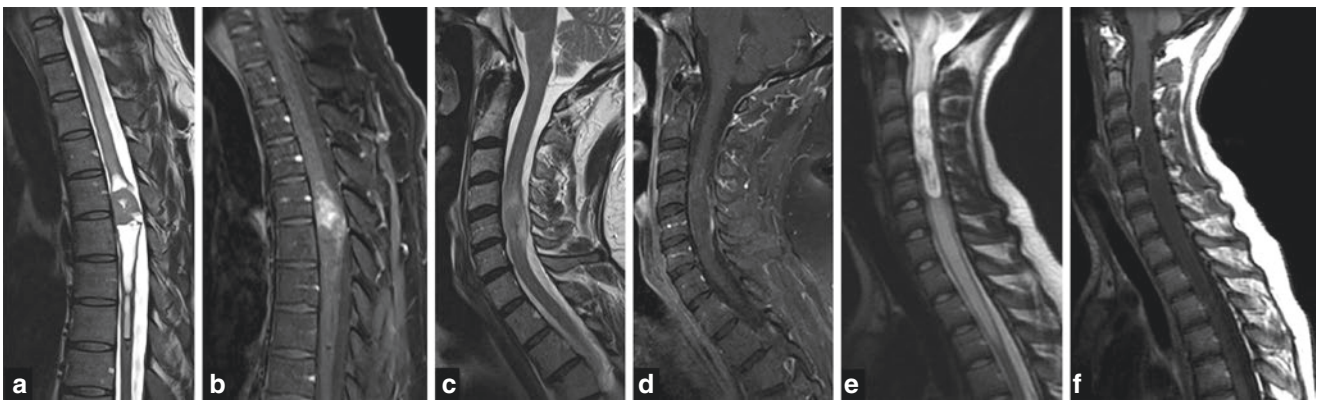

Fig. 18.15 (**a**) Sagittal T2WI and (**b**) contrast-enhanced T1WI shows an intramedullary expansile mass with central, irregular enhancing nodularity and polar cysts. The inferior hemosiderin cap favors ependymoma. (**c**) Sagittal T2WI and (**d**) contrast-enhanced T1WI demonstrates an intramedullary infiltrative mass with ill-defined patchy enhancement, features which suggest astrocytoma. (**e**) Sagittal T2WI and (**f**) contrast-enhanced T1WI shows a hemangioblastoma with the characteristic punctate enhancing nodule along the anterior cord associated with a large cyst and extensive edema

intramedullary neoplasms to consider are ependymoma, astrocytoma, and hemangioblastoma. In patients with history of malignancy, metastases should be in the differential diagnosis.

Ependymoma is the most frequently encountered glial tumor in adults, while astrocytoma is the most common glial tumor in the pediatric population. Ependymomas are sharply defined, variable enhancing, encapsulated tumors, which are usually central in location. These tumors commonly demonstrate peritumoral cystic change and hemorrhage. The hemosiderin "cap" sign is seen in 20–30% of cases and is a helpful clue to the diagnosis [27]. In contradistinction, astrocytomas have a poorly defined, infiltrative appearance often involving multiple vertebral body levels and sometimes the entire spinal cord [27]. There is often patchy enhancement and peritumoral edema. Hemangioblastomas are nonglial tumors with the typical appearance of an avidly enhancing nodule with or without an associated tumor cyst or syrinx formation. Large hemangioblastomas may show adjacent serpentine flow voids from prominent feeding vessels (Fig. 18.15). Intramedullary spinal cord metastasis may show features on postgadolinium images to help distinguish them from primary cord masses: the "rim" sign (more intense thin rim of peripheral enhancement around an enhancing lesion) and the "flame" sign (ill-defined flame-shaped region of enhancement at the superior/inferior lesion margins) (Fig. 18.16). Either or both signs have high specificity (97% and 100%, respectively) [28].

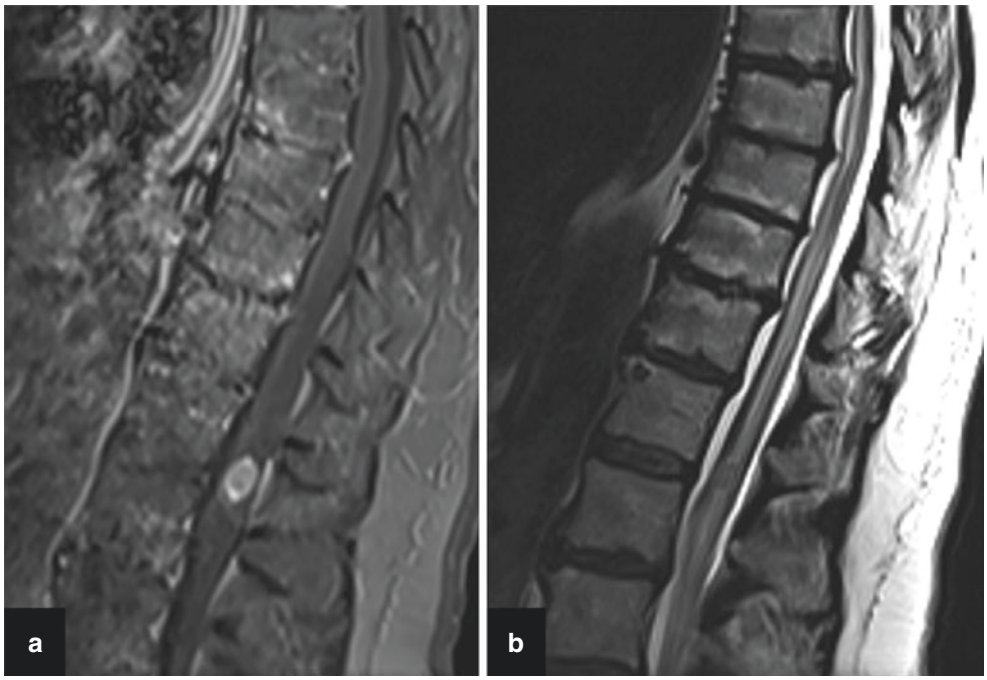

Fig. 18.16 (**a**) Sagittal contrast-enhanced T1WI and (**b**) T2WI demonstrate an intramedullary spinal cord metastasis. The lesion shows more intense thin rim of peripheral enhancement and ill-defined flame-shaped region of enhancement at the inferior margin. Extensive intramedullary T2 hyperintensity extends superiorly due to cord edema

18.3 Radiculopathy

When evaluating the imaging for a patient with radiculopathy, degenerative changes affecting spinal nerves are the leading consideration followed by infectious and inflammatory processes. Pathologies involving the brachial and lumbosacral plexus can also present as radiculopathy.

Degenerative lesions, such as disc herniations (protrusion, extrusion) and endplate osteophytes can impinge on the exiting nerve roots in the neural foramina and on the transiting nerve roots in the subarticular zones. Patients will present with radicular symptoms in a distinct nerve distribution. Other degenerative processes that cause nerve impingement include synovial cysts (Fig. 18.17), facet or uncovertebral osteophytes, and segmental motion with instability. The latter may not be appreciated on supine imaging and upright radiographs with axial loading provides complementary functional information. Findings of degenerative isthmic spondylothesis and facet hypertrophy with facet effusions suggests segmental motion [29].

Inflammatory lesions that involve the cauda equina nerves can present with neurological symptoms that can be difficult to differentiate clinically from myelopathy. One such entity that is a common cause of acute flaccid paralysis is acute inflammatory demyelinating polyneuropathy (AIDP)/Guillain-Barré syndrome. AIDP is an immune-mediated polyradiculoneuropathy that presents with acute ascending limb weakness associated with reduced reflexes. There is often history of a preceding infective illness [30]. Extremity weakness progresses, which can last up to 4 weeks before reaching plateau. The disease may progress in some patients, causing autonomic dysfunction, bulbar weakness, and respiratory insufficiency. Acutely, the cauda equina nerves may show thickening and enhancement on MRI, which has a sensitivity of 83% [31]. Classically, there may be anterior root involvement although both anterior and posterior roots may be involved. Chronic inflammatory demyelinating polyneuropathy (CIDP) is an indolent demyelinating pathology with symptoms beyond 8 weeks. Patients may present with posterior column sensory signs (e.g., ataxia, vibratory, or proprioceptive loss). On MRI, the brachial plexus, lumbosacral plexus, and cauda equina nerves may be diffusely enlarged and show mild enhancement (Fig. 18.18). Additionally, the muscles, supplied by the nerves, will demonstrate denervation changes: mild enhancement and T2 hyperintensity acutely/subacutely and fatty atrophy chronically.

Neoplastic processes from primary or secondary tumors can metastasize to the leptomeninges, resulting in leptomeningeal carcinomatosis. The subarachnoid spread of malignant cells may be "drop metastases" from primary CNS tumors or via hematogenous spread. The imaging appearance of leptomeningeal metastatic disease is variable, from thin and linear to thick and nodular enhancement (sugar coating).

Spinal nerve sheath tumors as schwannoma and neurofibroma can be intradural extramedullary in location or may involve the brachial and lumbosacral plexi. Schwannomas are often solitary and sporadic, presenting initially with radicular pain followed by motor weakness, voiding difficulty, and myelopathy. These globular, well-defined, encap-

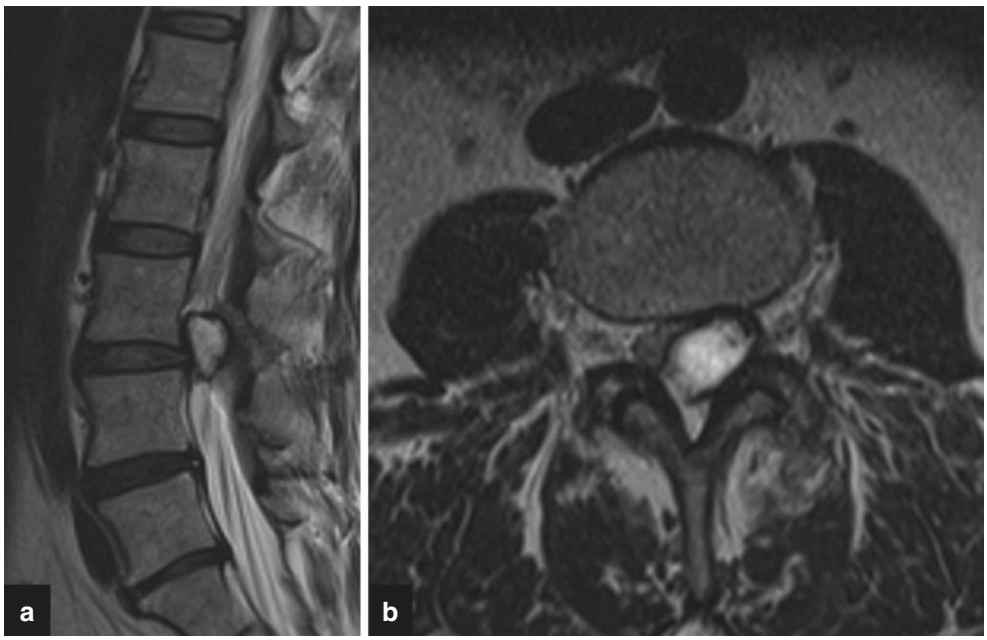

Fig. 18.17 (**a**) Sagittal and (**b**) axial T2WI show a synovial cyst with the classic T2 hypointense rim, protruding anteromedially from the left L3/L4 facet joint. The impinges on the transiting L4 nerve as well as compresses the thecal sac

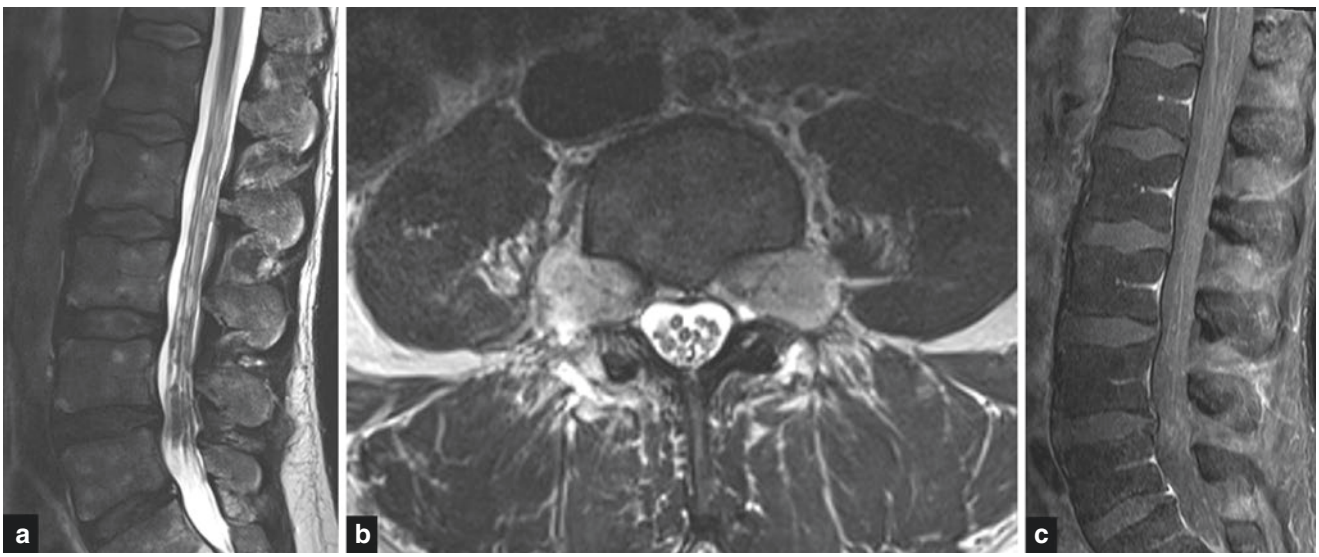

Fig. 18.18 (**a**) Sagittal and (**b**) axial T2WI shows thickened cauda equina nerves. The exiting nerves are mildly T2 hyperintense and markedly enlarged. (**c**) Sagittal contrast-enhanced T1WI demonstrates mild enhancement of the thickened cauda equina nerves

sulated tumors arise from Schwann cells of a sensory nerve root. Most spinal schwannomas are intradural extramedullary in location with adjacent osseous remodeling. Schwannomas and neurofibromas can appear very similar on MRI: T1 isointense, T2 hyperintense, enhancement. Some distinguishing features of schwannomas are hemorrhage, intrinsic vascular changes (thrombosis, sinusoidal dilatation), cyst formation, and fatty degeneration. Neurofibromas are often asymptomatic but may present with pain and/or radicular sensory changes. These lesions are hypodense on CT and cause smooth scalloping of the adjacent bone. On T2WI, neurofibromas may show a target sign: central low signal of collagenous stroma with hyperintense rim (Fig. 18.19).

Malignant peripheral nerve sheath tumors are rare and often associated with neurofibromatosis 1 (25–50% of cases) [32]. Clinical presentation includes new pain, weakness, and rapidly growing mass. On imaging, it can be difficult to differentiate malignant peripheral nerve sheath tumors from neurofibromas, particularly in patients with neurofibromatosis 1. MRI features that suggest malignant peripheral nerve sheath tumor are increased largest dimension of the mass,

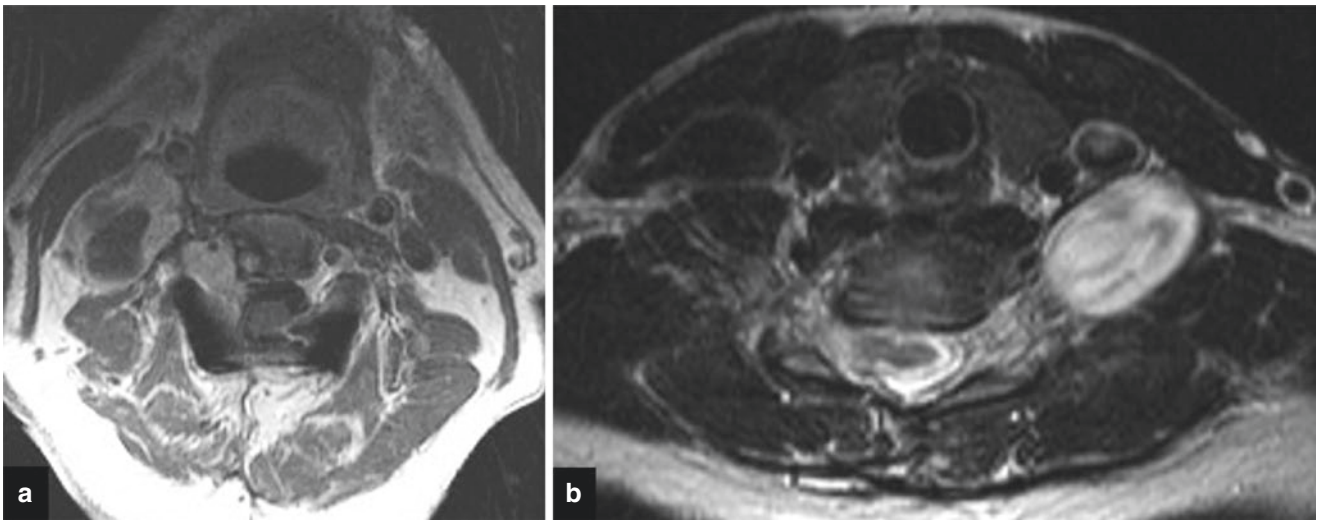

Fig. 18.19 (**a**) Axial contrast-enhanced T1WI of a dumbbell-shaped schwannoma shows heterogeneous enhancement with central cystic change and peripheral thick enhancement. (**b**) Axial T2WI of an extradural neurofibroma demonstrates hyperintensity with internal curvilinear hypointensity related to collagenous stroma

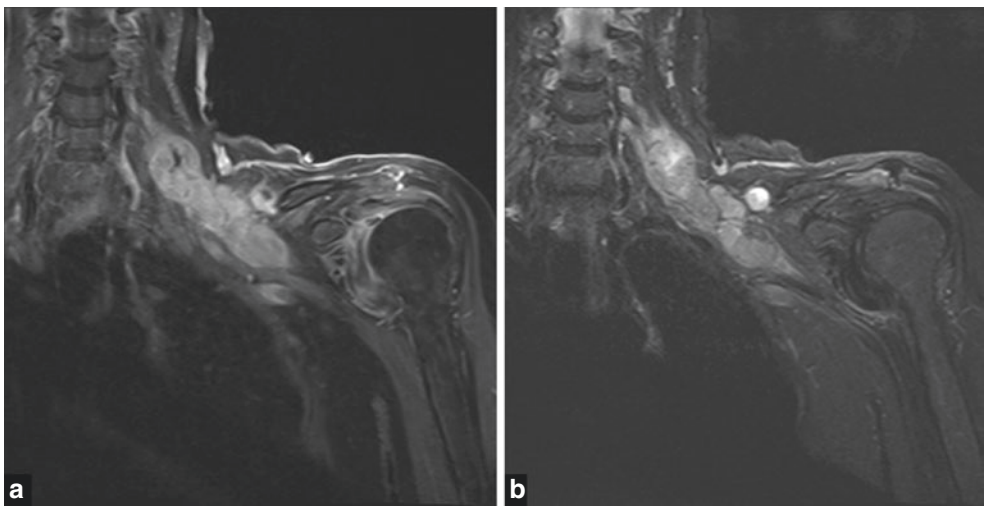

Fig. 18.20 (**a**) Coronal contrast-enhanced T1WI and (**b**) STIR MRI show an intensely enhancing malignant nerve sheath tumor arising from the lower left brachial plexus infiltrating along the trunks, divisions, and cords

presence of peripheral enhanced pattern, presence of perilesional edema-like zone, presence of intratumoral cystic lesion, and heterogeneity on the T1-weighted images (particularly in patients with neurofibromatosis 1) (Fig. 18.20). One study found the presence of two or more of the four features suggests malignancy with a sensitivity of 61% and a specificity of 90% [32]. FDG-PET uptake can be an essential component of diagnosis of malignant transformation of peripheral nerve sheath tumors.

Key Point

- Intradural extramedullary nerve sheath tumors can press upon spinal nerves and/or the spinal cord and result in radicular and myelopathic symptoms, respectively.

18.4 Concluding Remarks

A spectrum of spine pathologies can result in myelopathy and/or radiculopathy. Integrating the clinical features, temporal course, and anatomic distribution with the imaging characteristics, particularly on MRI, is important in narrowing the differential diagnosis or establishing a definitive diagnosis.

Take-Home Messages

- Extrinsic lesions such as DCM, meningiomas, and epidural hematoma can cause neurologic symptoms due to compression of the spinal cord.
- Imaging findings can be valuable in differentiating between lesions that cause ventral cord displacement: cord herniation, arachnoid web, and arachnoid cyst.
- The MRI pattern combined with the temporal presentation and clinical signs and symptoms can help narrow the differential considerations of intrinsic spinal cord lesions.
- Breakdown of the blood–cord barrier resulting in spinal cord enhancement can be seen a variety of pathologies including infections, inflammation, demyelination, and neoplastic.
- Clues to the diagnosis of spinal cord pathology may lie in the surrounding soft tissues or bones.

References

1. Wilson JRF, Badhiwala JH, Moghaddamjou A, Martin AR, Fehlings MG. Degenerative cervical myelopathy; a review of the latest advances and future directions in management. Neurospine. 2019;16(3):494–505.
2. Vedantam A, Rajshekhar V. Does the type of T2-weighted hyperintensity influence surgical outcome in patients with cervical spondylotic myelopathy? A review. Eur Spine J. 2013;22(1):96–106.
3. Flanagan EP, Krecke KN, Marsh RW, Giannini C, Keegan BM, Weinshenker BG. Specific pattern of gadolinium enhancement in spondylotic myelopathy. Ann Neurol. 2014;76(1):54–65.
4. Boden SD, McCowin PR, Davis DO, Dina TS, Mark AS, Wiesel S. Abnormal magnetic-resonance scans of the cervical spine in asymptomatic subjects. A prospective investigation. J Bone Joint Surg Am. 1990;72(8):1178–84.
5. Matsumoto M, Okada E, Ichihara D, et al. Age-related changes of thoracic and cervical intervertebral discs in asymptomatic subjects. Spine. 2010;35(14):1359–64.
6. Holtas S, Heiling M, Lonntoft M. Spontaneous spinal epidural hematoma: findings at MR imaging and clinical correlation. Radiology. 1996;199(2):409–13.
7. Fukui MB, Swarnkar AS, Williams RL. Acute spontaneous spinal epidural hematomas. AJNR Am J Neuroradiol. 1999;20(7):1365–72.
8. Atlas SW, DuBois P, Singer MB, Lu D. Diffusion measurements in intracranial hematomas: implications for MR imaging of acute stroke. AJNR Am J Neuroradiol. 2000;21(7):1190–4.
9. Mauch JT, Carr CM, Cloft H, Diehn FE. Review of the imaging features of benign osteoporotic and malignant vertebral compression fractures. AJNR Am J Neuroradiol. 2018;39(9):1584–92.
10. Koeller KK, Shih RY. Intradural extramedullary spinal neoplasms: radiologic-pathologic correlation. Radiographics. 2019;39(2):468–90.
11. Reardon MA, Raghavan P, Carpenter-Bailey K, et al. Dorsal thoracic arachnoid web and the "scalpel sign": a distinct clinical-radiologic entity. AJNR Am J Neuroradiol. 2013;34(5):1104–10.
12. Schultz R Jr, Steven A, Wessell A, et al. Differentiation of idiopathic spinal cord herniation from dorsal arachnoid webs on MRI and CT myelography. J Neurosurg Spine. 2017;26(6):754–9.
13. Kearney H, Miller DH, Ciccarelli O. Spinal cord MRI in multiple sclerosis--diagnostic, prognostic and clinical value. Nat Rev Neurol. 2015;11(6):327–38.
14. Pekcevik Y, Mitchell CH, Mealy MA, et al. Differentiating neuromyelitis optica from other causes of longitudinally extensive transverse myelitis on spinal magnetic resonance imaging. Mult Scler. 2016;22(3):302–11.
15. Yonezu T, Ito S, Mori M, et al. "Bright spotty lesions" on spinal magnetic resonance imaging differentiate neuromyelitis optica from multiple sclerosis. Mult Scler. 2014;20(3):331–7.
16. Dos Passos GR, Oliveira LM, da Costa BK, et al. MOG-IgG-associated optic neuritis, encephalitis, and myelitis: lessons learned from neuromyelitis optica spectrum disorder. Front Neurol. 2018;9:217.
17. Ciccarelli O, Cohen JA, Reingold SC, et al. Spinal cord involvement in multiple sclerosis and neuromyelitis optica spectrum disorders. Lancet Neurol. 2019;18(2):185–97.
18. Bathla G, Singh AK, Policeni B, Agarwal A, Case B. Imaging of neurosarcoidosis: common, uncommon, and rare. Clin Radiol. 2016;71(1):96–106.
19. Hashmi M, Kyritsis AP. Diagnosis and treatment of intramedullary spinal cord sarcoidosis. J Neurol. 1998;245(3):178–80.
20. Zalewski NL, Krecke KN, Weinshenker BG, et al. Central canal enhancement and the trident sign in spinal cord sarcoidosis. Neurology. 2016;87(7):743–4.
21. Talbott JF, Narvid J, Chazen JL, Chin CT, Shah V. An imaging-based approach to spinal cord infection. Semin Ultrasound CT MR. 2016;37(5):411–30.
22. Novy J, Carruzzo A, Maeder P, Bogousslavsky J. Spinal cord ischemia: clinical and imaging patterns, pathogenesis, and outcomes in 27 patients. Arch Neurol. 2006;63(8):1113–20.
23. Hurst RW, Grossman RI. Peripheral spinal cord hypointensity on T2-weighted MR images: a reliable imaging sign of venous hypertensive myelopathy. AJNR Am J Neuroradiol. 2000;21(4):781–6.
24. Badhiwala JH, Farrokhyar F, Alhazzani W, et al. Surgical outcomes and natural history of intramedullary spinal cord cavernous malformations: a single-center series and meta-analysis of individual patient data: clinic article. J Neurosurg Spine. 2014;21(4):662–76.
25. Larner AJ, Zeman AZ, Allen CM, Antoun NM. MRI appearances in subacute combined degeneration of the spinal cord due to vitamin B12 deficiency. J Neurol Neurosurg Psychiatry. 1997;62(1):99–100.
26. Marelli C, Salsano E, Politi LS, Labauge P. Spinal cord involvement in adult-onset metabolic and genetic diseases. J Neurol Neurosurg Psychiatry. 2019;90(2):211–8.
27. Koeller KK, Rosenblum RS, Morrison AL. Neoplasms of the spinal cord and filum terminale: radiologic-pathologic correlation. Radiographics. 2000;20(6):1721–49.
28. Rykken JB, Diehn FE, Hunt CH, et al. Rim and flame signs: post-gadolinium MRI findings specific for non-CNS intramedullary spinal cord metastases. AJNR Am J Neuroradiol. 2013;34(4):908–15.

29. Aggarwal A, Garg K. Lumbar facet fluid-does it correlate with dynamic instability in degenerative spondylolisthesis? A systematic review and meta-analysis. World Neurosurg. 2021;149:53–63.
30. Jacobs BC, Rothbarth PH, van der Meche FG, et al. The spectrum of antecedent infections in Guillain-Barre syndrome: a case-control study. Neurology. 1998;51(4):1110–5.
31. Gorson KC, Ropper AH, Muriello MA, Blair R. Prospective evaluation of MRI lumbosacral nerve root enhancement in acute Guillain-Barre syndrome. Neurology. 1996;47(3):813–7.
32. Wasa J, Nishida Y, Tsukushi S, et al. MRI features in the differentiation of malignant peripheral nerve sheath tumors and neurofibromas. AJR Am J Roentgenol. 2010;194(6):1568–74.